

Review Article

Cellular Potts modeling of complex multicellular behaviors in tissue morphogenesis

Tsuyoshi Hirashima,^{1*}  Elisabeth G. Rens^{2,3} and Roeland M. H. Merks^{2,3}

¹Institute for Frontier Life and Medical Sciences, Kyoto University, 53 Kawahara, Shogoin, Sakyo-ku, Kyoto 606-8507 Japan; ²Centrum Wiskunde & Informatica, Life Sciences Group, Science Park 123, 1098 XG, Amsterdam; and ³Mathematical Institute, Leiden University, Niels Bohrweg 1, 2333 CA, Leiden, the Netherlands

Mathematical modeling is an essential approach for the understanding of complex multicellular behaviors in tissue morphogenesis. Here, we review the cellular Potts model (CPM; also known as the Glazier-Graner-Hogeweg model), an effective computational modeling framework. We discuss its usability for modeling complex developmental phenomena by examining four fundamental examples of tissue morphogenesis: (i) cell sorting, (ii) cyst formation, (iii) tube morphogenesis in kidney development, and (iv) blood vessel formation. The review provides an introduction for biologists for starting simulation analysis using the CPM framework.

Key words: blood vessel formation, cellular Potts model, cystogenesis, tube morphogenesis.

Introduction

Biological tissue architectures emerge as a consequence of complex multicellular behaviors during embryonic development. With the molecular insight provided by genetic experiments, ever-improving visualization techniques including microscopy systems and fluorescence tools have revealed multicellular behaviors associated with the spontaneous formation of structures and patterns from the cell to the whole-organ scale (Abe & Fujimori 2013; Keller 2013; Chen *et al.* 2014; Miyawaki & Niino 2015). These techniques are the basis of quantification of chemico-mechanical activities in intra- and inter-cellular regulation of developing tissues (Grashoff *et al.* 2010; Aoki *et al.* 2013; Polacheck & Chen 2016; Serwane *et al.* 2016). Hence, it is expected that a large amount of data on multicellular dynamics can be accumulated. Instead of listing the activities of constituent cells, integrating interconnections of those cellular activities into a mechanistic mathematical modeling framework is an effective approach towards understanding how complex multicellular behaviors drive the formation of tissue architectures (Kitano 2002; Merks & Glazier 2005; Sasai 2013).

In this review, we introduce the cellular Potts model (CPM), a ‘cell-centered’ modeling framework that has been employed to represent complex multicellular behaviors. Our aim is to describe its usability for modeling various developmental phenomena to biologists that are new to modeling by presenting applications without mathematical details. Following a brief explanation of the CPM, we provide guidance for biologists who want to analyze their system using CPM simulations along four typical applications of the CPM to tissue morphogenesis: (i) cell sorting, (ii) cyst formation, (iii) tube morphogenesis, and (iv) blood vessel formation.

Cellular Potts model

The CPM, also known as the Glazier-Graner-Hogeweg (GGH) model, is a cell-based computational modeling framework and has been utilized to describe complex cell behaviors (Graner & Glazier 1992; Glazier & Graner 1993; Hogeweg 2000). The CPM represents biological cells on a regular lattice as usually connected domains of lattice sites identified with the same numerical index. This representation enables the CPM to express arbitrary cell shapes (Fig. 1A). The domains in the general CPM framework can also represent other biological structures, including subcellular compartments or the extracellular matrix (Starruß *et al.* 2007; Boas & Merks 2014; Dias *et al.* 2014). Because the

*Author to whom all correspondence should be addressed.

Email: hirashima.tsuyoshi.2m@kyoto-u.ac.jp

Received 13 March 2017; accepted 24 March 2017.

© 2017 Japanese Society of Developmental Biologists

biological structures can be flexibly represented on regular lattices, the CPM can be conveniently interfaced with simulations of a range of physical processes, including reactions within cells, diffusion in extracellular space, and the mechanics of the extracellular matrix (Angermann *et al.* 2012; Albert & Schwarz 2014, 2016; van Oers *et al.* 2014; Rens & Merks 2017). Owing to its straightforward expression of cell shape and cell motility, the CPM is regarded as a convenient modeling tool to dynamically describe cell behavior and tissue structures across multiple scales (Fig. 1B).

The cell behavior in the CPM depends on a balance of forces described by a generalized energy H . In the basic form of the CPM, H is a sum of the interfacial energies and energies due to the cell's deviation from a resting volume. The interfacial

energies are due to intercellular adhesion and other sources of interfacial tension at intercellular and cell-matrix boundaries, including cortical tension (Krieg *et al.* 2008). The mathematical details are described elsewhere (Graner & Glazier 1992; Glazier & Graner 1993; Ouchi *et al.* 2003). The dynamics proceed stochastically on the basis of a free energy minimization using a dynamic Monte Carlo simulation algorithm. To mimic pseudopod extensions and retractions of the cells, this algorithm randomly selects a lattice site (source site) and attempts to copy its index into a randomly chosen neighboring site (target site). If this site belongs to a different biological cell (i.e., if it has a different index), the algorithm checks the net energy changes associated with this move (Fig. 1C). While the index copying occurs in a deterministic manner for the case of energy

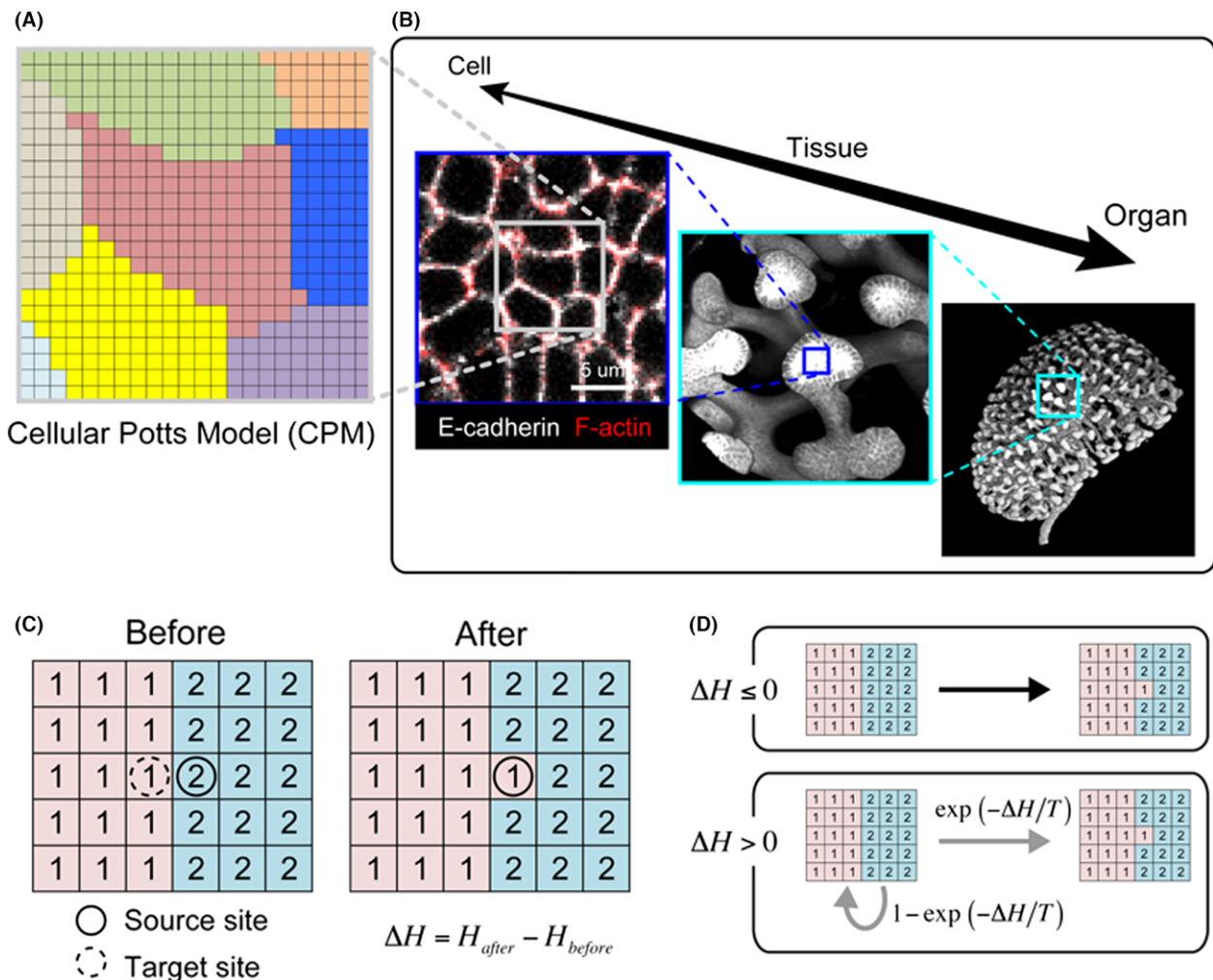


Fig. 1. Cellular Potts model (CPM). (A) On-lattice expression in the CPM. Colors represent individual cells. (B) Multiple scales from cells to organs in living structure. (C) Configuration change by the index copying. (D) Rule of state transitions in the CPM. $\Delta H = H_{\text{after}} - H_{\text{before}}$. (O): Source site; (⊖): Target site).

decrease, it occurs stochastically with the following Boltzmann acceptance function for the case of energy increase (Fig. 1D):

$$\Pr \left[\begin{array}{l} \text{transition} \\ \text{accepted} \end{array} \right] = \begin{cases} 1 & \text{if } \Delta H \leq 0 \\ \exp(-\Delta H/T) & \text{if } \Delta H > 0 \end{cases}$$

where T represents a simulation temperature that determines the magnitude of random biological fluctuations. A higher T causes large fluctuations allowing mesenchymal-like cell behaviors. For extremely high T (melting temperature), the cells tend to disintegrate as the system becomes dominated by random fluctuations. The naïve algorithm described above can be sped up using a variety of techniques developed for related, kinetic Monte Carlo methods (Newman & Barkema 1999). For example, rejection-free algorithms maintain a list of lattice site pairs at the cell–cell interfaces to prevent the repetitive selection and rejection of lattice site of identical index; due to the computational cost of maintaining such lists, these algorithms become particularly favorable for CPM configurations with high surface-volume ratios. Other authors have proposed synchronous update schemes to speed up the CPM (Harrison *et al.* 2011); we recommend against using these, as they may change the systems kinetics.

The series of index-copies attempts to reach an energetic global minimum corresponding to force-balance, if it exists. This is, to some extent, compatible with the over-damped dynamics of *in vivo* environments, in which viscosity dominates inertia and the effective force, acting on cells is proportional to the velocity of the cells (Merks & Glazier 2005; Marée *et al.* 2007; Swat *et al.* 2012). However, it should be noted that the validity of the dynamics in the CPM becomes unclear for cases when the state of the system is moving far from the mechanical equilibrium due to, for example, constant injection of energy into the system.

An advantage of the CPM is its simplicity in implementing various cellular activities, such as shape change, active contraction, proliferation, and apoptosis, and the users can examine the influences of cell-level events on multicellular tissues (Zajac *et al.* 2000, 2003; Merks *et al.* 2006; Akanuma *et al.* 2016; Belmonte *et al.* 2016). Additionally, because of its extensibility, the CPM allows us to tackle issues in a wide spectrum of biological phenomena including biomedical applications, e.g., cancer biology and wound healing (Savill & Merks 2007; Hirashima *et al.* 2013; Szabó & Merks 2013; Noppe *et al.* 2015). Please refer to other reviews for additional applications and details regarding the model (Merks & Glazier 2005; Balter

et al. 2007; Marée *et al.* 2007; Scianna & Preziosi 2012; Swat *et al.* 2012; Szabó & Merks 2013). See (Glazier *et al.* 2007) for details about the historical origins of the CPM.

There is a growing demand for biologists to use mathematical models for predictions or generating a working hypothesis in their research. To do so, biologists should be able to perform simulation analysis using multicellular models by themselves. Without devoting to writing source codes, open source simulation environments like *CompuCell3D* or *Morpheus* support the entire workflow of the computational model analysis with graphical user interfaces depending on settings of individual users (Swat *et al.* 2012; Staruß *et al.* 2014). Moreover, open source C++ libraries are available (e.g., Tissue Simulation Toolkit, see (Daub & Merks 2014)). These environments assist biologists in their *in silico* analysis to better understand complex multicellular behaviors in tissue morphogenesis.

CPM applications in tissue morphogenesis

Cell sorting

A well-studied biological phenomenon that has been successfully explained using the CPM is cell sorting (Graner & Glazier 1992; Glazier & Graner 1993; Steinberg 2007). Cell sorting spontaneously occurs through rearrangement of cells or selective cell aggregation in various developmental processes (Townes & Holtfreter 1955; Krens & Heisenberg 2011). To understand the mechanisms underlying the sorting behavior of cells, biophysical aspects of the phenomenon have been studied experimentally and theoretically since Steinberg proposed the differential adhesion hypothesis (DAH), i.e., the sorting of embryonic tissues results from differences in intercellular adhesion (Steinberg 1963, 2007; Steinberg & Takeichi 1994; Brodland 2004; Foty & Steinberg 2005). Recently, the mechanical factors driving cell sorting have begun to be clarified; cell sorting depends on the coupling function generated through mechanical anchoring of adhesion molecules to the cell cortex between intercellular surface tension due to the cell–cell adhesion and cortical tension (Lecuit & Lenne 2007; Heisenberg & Bellaïche 2013).

Simulations of the CPM incorporating the mechanical factors are sufficient to reproduce the multicellular patterns that emerge as a result of the cell sorting observed in experiments (Käfer *et al.* 2007; Krieg *et al.* 2008). In these simulations, in addition to interfacial energies originating from cell–cell adhesion, the Hamiltonian includes a cortical tension term (Ouchi *et al.* 2003). Although CPMs based on the DAH alone can explain separation of differentially-adherent cells,

cortical tension terms are required for sorting in the biologically correct order (Glazier *et al.* 2007; Magno *et al.* 2015) and can affect the kinetics of cell sorting (Nakajima & Ishihara 2011). Further insights into the dynamic aspects of cell sorting will become available after more experimental data are integrated into CPM simulations.

Cyst formation

In recent years, advanced computer performance has made it possible to study the formation of 3D multicellular structures using the CPM. Particularly, cystogenesis is an appropriate target to understand how epithelial cells coordinate their polarity in space and time to form a spherical monolayer that has a single fluid-filled lumen in 3D extracellular matrix (Fig. 2A). *In vitro* studies have revealed that cells involved in cystogenesis acquire apico-basal polarity during the process, and several cellular activities including proliferation and migration involved in maintaining cell-cell adhesion are coordinated to generate the spherical structure polarized on a tissue scale (Bryant & Mostov 2008; Martin-Belmonte & Mostov 2008). Therefore,

understanding dynamical aspects in the activities of individual polarized cells is essential for clarifying mechanisms underlying the generation of epithelial cysts.

For implementing the polarity of individual cells, sub-cellular compartments are introduced into the cells in the CPM. For example, modeling the apical region in the cells at the cell-lumen interface in the cyst leads to representing the dynamics of individual polarized cells (Fig. 2B). Based on this framework, Cerruti *et al.* (2013) modeled the cystogenesis of Madin-Darby canine kidney (MDCK) cells, which have served as an excellent *in vitro* experimental system for cystogenesis, and analyzed their CPM to reveal what generates multi-lumen structures appearing in abnormal cystogenesis. They examined the relationship between doubling time in cell division and relaxation time of the system to its mechanical equilibrium during cystogenesis, and found that the multilumen structures tend to appear when the doubling time is shorter than the relaxation time (Fig. 2C). This can be regarded as a consequence of aberrant cell proliferation due to the loss of contact inhibition (Abercrombie 1979). In addition to the extreme cell proliferation, Belmonte *et al.* used the

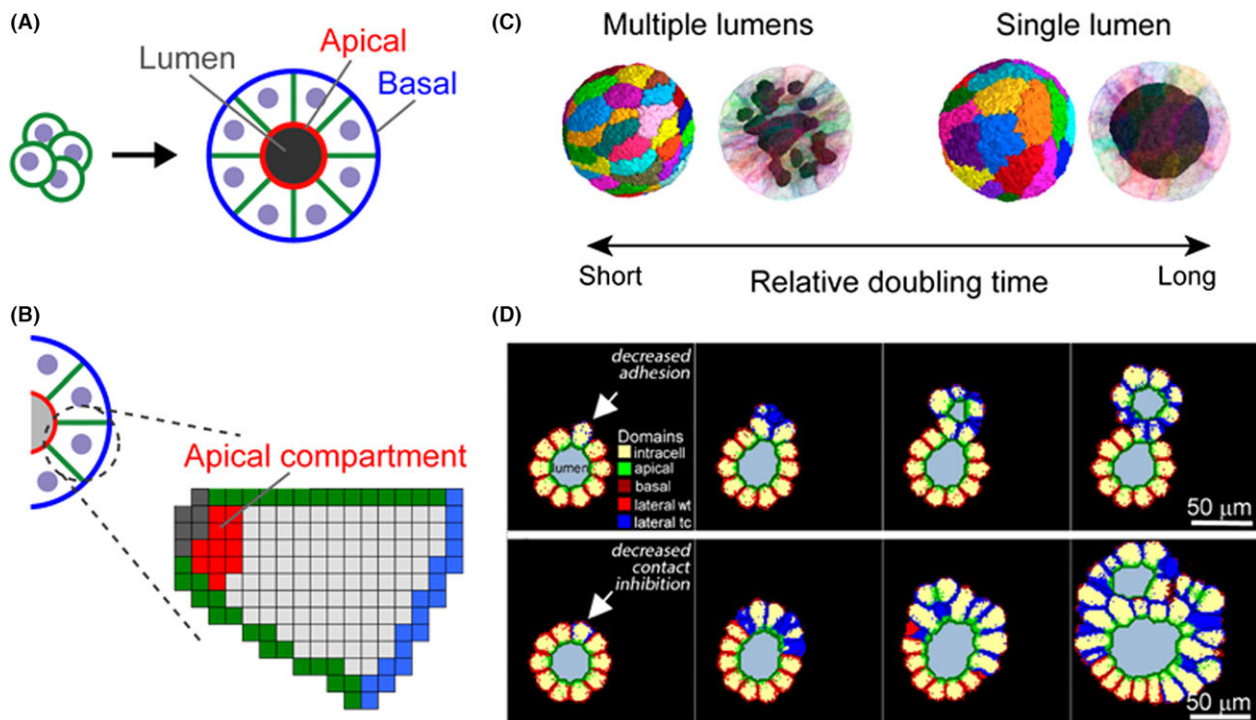


Fig. 2. Cyst formation. (A) Schematics for cystogenesis. (B) Representation of cells and subcellular compartments in the cellular Potts model (CPM). (C) Lumen formation in cysts depending on the relative doubling time of constituent cells. Parts of C are reproduced from ©Cerruti *et al.* 2013; published in *Journal of Cell Biology*. (D) Ectopic cyst induction by either decreased adhesion or decreased contact inhibition. Reproduced from Belmonte *et al.* 2016 with permission from the American Society for Cell Biology. Originally published in *Molecular Biology of the Cell*.

CPM to predict that a reduction in cell–cell adhesion in an epithelial monolayer of the polarized multicellular structure triggers ectopic cyst induction, eventually producing multilumens, and verified the model prediction *in vitro* (Belmonte *et al.* 2016) (Fig. 2D). By integrating predictive CPM modeling and experimental validation, these studies have deepened the understanding of how genetic mutations can trigger cystic diseases by inducing subtle changes in cell behavior.

In addition to cellular compartments, the CPM can be used to examine non-cellular materials. Boas and Merks modeled intracellular vesicles and vacuoles in endothelial cells to examine mechanisms of lumen formation during blood vessel development (Boas & Merks 2014). They compared two competing explanations of lumen formation in blood vessels: (i) fusion of intracellular vacuoles transported out of the cells; and (ii) active repulsion of adjacent cells. Extensive simulation studies for broad parameter ranges led them to conclude that only simultaneous operation of the two mechanisms would robustly produce lumens. By thus extending the CPM to describe chemico-mechanical factors, we can better understand dynamic properties of cells during the lumen formation.

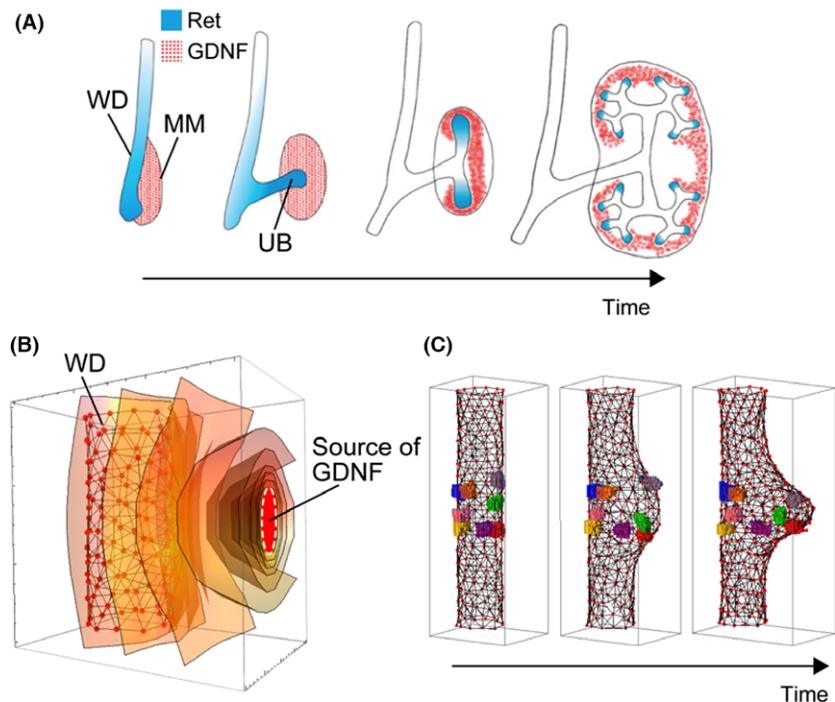
Tube morphogenesis

The CPM has been adopted to model tissue growth and deformation of relatively simple multicellular structures during development, such as the outgrowth of

the limb bud (Savill & Hogeweg 1997; Marée & Hogeweg 2001; Popławski *et al.* 2007) and subsequent digit formation (Chaturvedi *et al.* 2005; Cickovski *et al.* 2005), and morphogenesis of the cellular slime mold *Dictyostelium discoideum* from aggregation of free-living amoebae and slug formation (Savill & Hogeweg 1997) to fruiting body formation (Marée & Hogeweg 2001). In these processes, chemical communication between different tissues plays a pivotal role, as in most types of tissue morphogenesis. Hence, modeling tissue morphogenesis using the CPM has demonstrated the capability of integrating the dynamics of diffusive chemicals and reacting cells as chemotactic behaviors (Savill & Hogeweg 1997). We here explore an application of the CPM in which chemical interaction between different tissues is incorporated to understand a simple tissue morphogenesis observed during vertebrate kidney development.

The morphogenesis of kidneys occurs through reciprocal inductive interactions between the ureteric bud (UB) and metanephric mesenchyme (MM) via GDNF/Ret signaling; the secreted protein glial cell-line-derived neurotrophic factor (GDNF) is expressed in the MM adjacent to the caudal Wolffian duct (WD) and its receptor Ret is expressed throughout the WD and in the distal tip of the UB (Costantini & Shakya 2006) (Fig. 3A). During the process of the mutual induction between these tissues, the UB is formed by budding from the WD and elongates to the MM region, initiating a number of iterative branching events (Michos 2009;

Fig. 3. Wolffian duct (WD) morphogenesis. (A) Morphogenetic process of development of the epithelial tube in the kidney. Reproduced from Costantini & Shakya (2006) originally published in *BioEssays* with permissions from Wiley. The text labels have been added to the original figure. (B) Spatial distribution of diffusible molecule glial cell-line-derived neurotrophic factor (GDNF) around the WD. The contour planes of diffusive GDNF concentrations are visualized. Only the center position of the cells in the WD are in the display. (C) Time course of ureteric bud (UB) budding. Only some cells in the tube are visualized in order to show the tube structure.



Costantini & Kopan 2010). It has been revealed that Ret-expressing cells in the WD exhibit chemotaxis against the GDNF, which drives the outgrowth of the UB (Sariola & Sainio 1997; Tang *et al.* 1998). Moreover, it is known that the process is controlled via positive feedback of GDNF/Ret signaling (Majumdar *et al.* 2003).

In the CPM, a tubular structure similar to the WD can be modeled by introducing apical subcellular compartments using the techniques for polarized cells introduced in the previous section, and the macroscopic physical process of GDNF including diffusion and decay can be calculated on the grids simultaneously with the dynamics of cells (Fig. 3B). Simulations in which chemotaxis of UB cells was integrated using techniques similar to those used in earlier studies (Savill & Hogeweg 1997) suggest that the UB budding can occur from the WD as cells migrating along the gradient of GDNF (Fig. 3C). In addition, further analysis incorporating the effect of GDNF/Ret feedback regulation realized the dynamic morphogenetic process from the budding to the elongation as observed (Hirashima, unpubl. data, 2011). Furthermore, by incorporating a second role of GDNF as a stimulator of cell proliferation in the ureteric epithelia (Pepicelli *et al.* 1997), the CPM simulations predict that the balance between chemotaxis and cell proliferation of UB would determine the branching morphology in a single tip of the UB (Hirashima *et al.* 2009). When the chemotaxis is influential over the cell proliferation provided by GDNF, the single UB morphology becomes kinked, and in the opposite case, it becomes bloated. In general, tissue morphogenesis involves multiple feedback regulation loops; the studies review above illustrate that the CPM is a convenient modeling framework to implement such complex events.

Blood vessel formation

The CPM has found much application in the study of vascular development. Blood vessel formation occurs throughout development and adulthood. During embryonic development, dispersed endothelial cells aggregate to form networks, a process called vasculogenesis (Eichmann *et al.* 2005). In adult organisms, new blood vessels sprout from pre-existing ones in a process called angiogenesis (Carmeliet 2005). Angiogenesis occurs in physiological processes, for example, during wound healing, or in pathological processes, for example, during tumor angiogenesis. In order to promote or inhibit angiogenesis in these processes, a better understanding of the mechanisms behind blood vessel formation is required.

Much like any developmental mechanism, blood vessel formation involves an intricate, multiscale interplay between processes occurring at the molecular scale, at the cellular scale, and at the tissue scale. This makes the CPM, in combination with techniques to model the subcellular scale and the cellular microenvironment, including the extracellular matrix, a suitable tool for modeling blood vessel formation.

Although much experimental research has been dedicated to unravel how endothelial cells form vascular networks, it is still not completely clear what cell behavior makes vasculogenesis possible. Mathematical modelers proposed various mechanisms for vasculogenesis by using the CPM.

One class of models proposed that the endothelial cells attract one another via an autocrinally secreted chemoattractant, for example, via vascular endothelial growth factors (VEGF) or small cytokines (Gamba *et al.* 2003). In a CPM model resembling the Keller-Segel equations (Keller & Segel 1970) for chemotaxis (Merks *et al.* 2008), this mechanism makes the cells aggregate into disconnected islands, suggesting that such autocrine chemoattraction does not suffice for vascular network formation. Two alternative, additional assumptions, however, allow stable network formation. A first model showed that networks can form via autocrine chemoattraction if the chemotaxis is contact-inhibited (Merks *et al.* 2008). A potential mechanism for such contact-inhibition of chemotaxis is modulation of the activity of the VEGFR2 receptor by VE-cadherin activity (Dejana 2004). Consistent with this hypothesis, treatment with anti-VE-cadherin antibodies in mouse allantois cultures could prevent network formation of endothelial cells (Merks *et al.* 2008), but alternative explanations for this observation, including loss of cell-cell adhesion, cannot be excluded.

An alternative model showed that autocrine chemoattraction can generate stable networks if the endothelial cells are elongated (Merks *et al.* 2006). Interestingly, a more recent CPM study showed that cell elongation alone, in the absence of chemotaxis, can induce network formation (Palm & Merks 2013). In this model, adhesive elongated cells form elongated structures that connect to each other. Because the clusters rotate very slowly, the network is not in equilibrium, but continues to evolve, ever more slowly towards equilibrium, a phenomenon called dynamical arrested. Another CPM study suggested that cells which preferentially adhere to elongated cell aggregates can also form networks (Szabo *et al.* 2007). This cell behavior was proposed based the experimental observation that cellular networks can form on bare, fibronectin-coated substrates, in continuously shaken culture bottles to prevent the formation of chemical or

tensile gradients in the ECM, thus preventing cell–cell communication. The authors proposed that an increased tension at elongated parts of the network could recruit cell–cell adhesion molecules.

These proposed mechanisms can be tested and validated using experimental data. Kohn-Luque *et al.* noted that the diffusion speed for VEGF that was assumed in (Merks *et al.* 2008) is generally much lower than the values reported for most VEGF isoforms *in vitro* (Köhn-Luque *et al.* 2011). By including binding of VEGF to the extracellular matrix in the CPM, it was suggested that VEGF is secreted by an underlying endodermic tissue. Then, endothelial cells secrete ECM that the VEGF binds to. It was assumed that endothelial cells are more attracted to ECM-bound than to soluble VEGF. This mechanism also predicts network dynamics (Köhn-Luque *et al.* 2011), suggesting that including interactions of cells with the ECM is vital for increasing our understanding of the mechanisms of vasculogenesis. More recent work by Van Oers *et al.* also modeled cell–matrix interaction in the CPM, but of a mechanical type (van Oers *et al.* 2014) (Fig. 4A). In this model, cells generate mechanical strains in the matrix by pulling on it. Then, based on

experimental observations of cell movements, the authors modeled cells that preferentially move along these mechanical strains. This mechanism was based on the experimental observation that by straining the matrix, cells stiffen the matrix and subsequently better attach to it. The underlying assumption is that focal adhesions, the bundles of integrins that bind cells to the matrix, grow to larger size on stiff matrices. This mechanism is sufficient to explain network formation and sprouting on compliant matrices.

The models described above (Merks *et al.* 2006, 2008; van Oers *et al.* 2014), and a further study (Szabó *et al.* 2012) can, besides vasculogenesis, also explain sprouting from cellular spheroids, an *in vitro* mechanism thought to be representative for the first steps of angiogenesis (Szabó *et al.* 2012).

Other CPM studies have focused specifically on sprouting from a pre-existing vessel. In particular, the role of cell–matrix interactions through chemical and mechanical interactions were investigated (Daub & Merks 2013) (Fig. 4B). Bauer *et al.* (2007, 2009) represented ECM fibers using the CPM and studied a system where the vessel sprouts up a VEGF gradient secreted by a tumor (Fig. 4C). The cells at the tip of

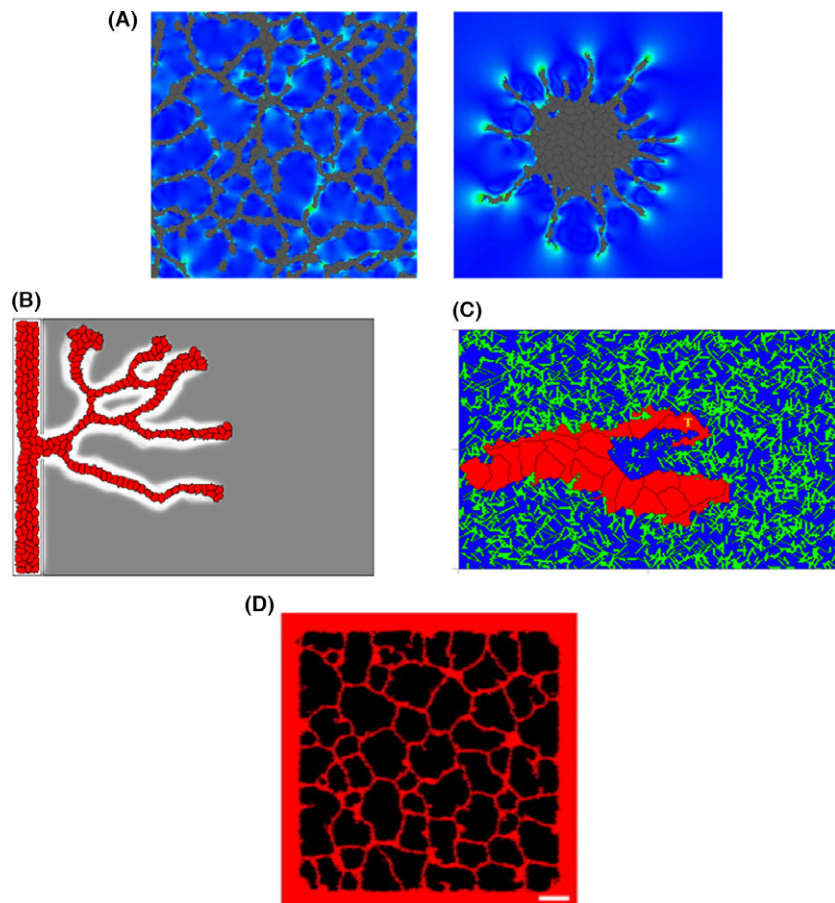


Fig. 4. Multiscale angiogenesis models. (A) Vascular network formation (left) and sprouting from a blob (left) and by mechanical cell–matrix interactions (van Oers *et al.* 2014). (B) Sprouting from a vessel into a matrix, branching is promoted by haptokineses (Daub & Merks 2013) (part of Fig. S1 in original). (C) Sprouting through a fibrous matrix by matrix degradation and chemotaxis towards a tumor (Bauer *et al.* 2009) (part of Fig. 7 in original). (D) Sprouting from a vessel produces vascular network in hypoxic region (Scianna *et al.* 2015) (part of Fig. 7 in original).

the sprout degrade the matrix and chemotact. This model suggests that due to haptotaxis, degradation and secreting of ECM, the speed, direction and the amount of branching depends on matrix fiber density. Daub and Merks also studied how a VEGF gradient and ECM density influences sprout dynamics (Daub & Merks 2013). In this model, cells secrete enzymes that degrade an ECM material, which was represented by a continuum field. The cells in this model exhibit chemotaxis, haptokinesis (migration speed proportional to ECM concentration) and haptotaxis (migration up non-diffusion ECM gradients). The authors found that haptokinesis promotes the formation of branches while haptotaxis primarily influenced the degree of sprouting.

In the model by Bauer *et al.* (2007), cells were given a fixed tip or stalk identity. Tip cells are generally more motile and responsive to VEGF, thus leading the sprout. Stalk cells are generally more proliferative and follow the tip cells. It is thought that tip and stalk cells do not maintain a fixed phenotype but can rapidly change phenotype through the Notch-Delta pathway. High intercellular Delta levels are associated with tip cells. Cell-cell signaling then reduces Delta in neighboring cells, which obtain a stalk phenotype. Such signaling can thus highly impact sprout progression. Prokopiou *et al.* (2016) studied sprout progression by means of chemotaxis and haptotaxis in the presence of Delta-Notch signaling. Simulation results of this model most closely mimic experimental data when the VEGF gradient is established by a VEGF secreting astrocytic cell and the fibrous matrix is heterogeneous.

(Scianna *et al.* (2015) studied sprouting from vessels in a hypoxic tissue (Fig. 4D). This model suggests that stalk cell proliferation perpendicular to sprouting is vital to optimal sprout progression. The formation of high vascularity in the hypoxic tissue is also stunted by interference of the Delta-Notch pathway. These multi-scale models show that cell-cell signaling and distinguishing of cell phenotypes are vital for a better understanding of angiogenesis.

Observations of tip and stalk cell motility in mouse embryoid bodies and mouse retina assays show that the tip cell position and role is repeatedly taken over by stalk cells further behind on the sprout (Jakobsson *et al.* 2010; Arima *et al.* 2011; Bentley *et al.* 2014; Sugihara *et al.* 2015). The function and mechanisms of this observed mechanism were not immediately clear and are subject to further studies. A combination of *in vitro* and *in vivo* imaging and mathematical modeling based on a modified CPM-model, has suggested that contact-dependent lateral inhibition via the Dll4-Notch pathway regulate active, polarized motion of candidate tip cells towards the tip position (Bentley *et al.* 2014). A recent CPM simulation study further

analyzed the two previous autocrine chemotaxis models of vasculogenesis and angiogenesis described above (Boas & Merks 2015). It was found that in these models overtake movements occur naturally, as a side-effect of the cell-cell interactions responsible for branching. Integrating a Dll4-Notch-VEGFR2 network in this model allowed cells at the tip to maintain the right phenotype. (Jakobsson *et al.* 2010; Bentley *et al.* 2014). This CPM study thus supports a view where, instead of being actively regulated by Notch levels, tip cell overtaking is a non-functional side-effect of the collective cell behavior that drives branching. In this view, Notch signaling acts to make tip-stalk patterning robust during branching (Jakobsson *et al.* 2010).

In conclusion, the CPM is able to reproduce the most important phenomenology of angiogenesis and vasculogenesis from relatively simple, experimentally plausible assumptions on endothelial cell behavior. By incorporating details on the subcellular scale and the microenvironment, more realistic tissue dynamics can be inferred and we can increase our understanding of how mechanisms working on different tissue scales and the intricate interplay among them may promote or inhibit blood vessel formation.

Perspectives

In this review, we showed application of the CPM to various multiscale phenomena of multicellular tissue development. The studies highlighted here take into account experimental facts, and hence, can be regarded as successful examples of how the model simulations contribute to bridging from complex interconnections of cellular activities to the processes of tissue morphogenesis. The CPM simulations are often not yet adequate to assimilate measured data with physical units (Marée *et al.* 2007; Oates *et al.* 2009), but other aspects including the kinetic exponents that characterize the dynamics of pattern formation can be readily matched with experiment data in order to validate if the model falls in the right universality class (Graner & Glazier 1992; Glazier & Graner 1993; Marée *et al.* 2007). The CPM has the advantage of incorporating information on complex multicellular phenomena without tricky algorithmic implementations. Therefore, it still provides an effective tool for biologists to interpret a large amount of spatio-temporal data for multicellular dynamics.

Acknowledgements

TH was supported by the Platform Project for Supporting in Drug Discovery and Life Science Research (Platform for Dynamic Approaches to Living System) from

Japan Agency for Medical Research and development (AMED), and by the JSPS KAKENHI grant 15K18541. RMHM and EGR were supported by the research program “Innovational Research Incentives Scheme Vidi Cross-divisional 2010 ALW” with project number 864.10.009, which is partly financed by the Netherlands Organization for Scientific Research (NWO).

References

- Abe, T. & Fujimori, T. 2013. Reporter mouse lines for fluorescence imaging. *Dev. Growth Differ.* **55**, 390–405.
- Abercrombie, M. 1979. Contact inhibition and malignancy. *Nature* **281**, 259–262.
- Akanuma, T., Chen, C., Sato, T., Merks, R. M. H. & Sato, T. N. 2016. Memory of cell shape biases stochastic fate decision-making despite mitotic rounding. *Nat. Commun.* **7**, 11963.
- Albert, P. J. & Schwarz, U. S. 2014. Dynamics of cell shape and forces on micropatterned substrates predicted by a cellular Potts model. *Biophys. J.* **106**, 2340–2352.
- Albert, P. J. & Schwarz, U. S. 2016. Dynamics of cell ensembles on adhesive micropatterns: bridging the gap between single cell spreading and collective cell migration. *PLoS Comput. Biol.* **12**, e1004863.
- Angermann, B. R., Klauschen, F., Garcia, A. D., Prustel, T., Zhang, F., Germain, R. N. & Meier-Schellersheim, M. 2012. Computational modeling of cellular signaling processes embedded into dynamic spatial contexts. *Nat. Methods* **9**, 283–289.
- Aoki, K., Kamioka, Y. & Matsuda, M. 2013. Fluorescence resonance energy transfer imaging of cell signaling from in vitro to in vivo: basis of biosensor construction, live imaging, and image processing. *Dev. Growth Differ.* **55**, 515–522.
- Arima, S., Nishiyama, K., Ko, T., Arima, Y., Hakozaki, Y., Sugi-hara, K., Koseki, H., Uchijima, Y., Kurihara, Y. & Kurihara, H. 2011. Angiogenic morphogenesis driven by dynamic and heterogeneous collective endothelial cell movement. *Development* (Cambridge, England) **138**, 4763–4776.
- Balter, A., Merks, R. M. H., Poplawski, N. J., Swat, M. & Glazier, J. A. 2007. The Glazier-Graner-Hogeweg Model: Extensions, Future Directions, and Opportunities for Further Study. *Single-Cell-Based Models in Biology and Medicine*, **2**, 17.
- Bauer, A. L., Jackson, T. L. & Jiang, Y. 2007. A cell-based model exhibiting branching and anastomosis during tumor-induced angiogenesis. *Biophys. J.* **92**, 3105–3121.
- Bauer, A. L., Jackson, T. L. & Jiang, Y. 2009. Topography of extracellular matrix mediates vascular morphogenesis and migration speeds in angiogenesis. A. Czirók, ed. *PLoS Comput. Biol.* **5**, e1000445.
- Belmonte, J. M., Clendenon, S. G., Oliveira, G. M., Swat, M. H., Greene, E. V., Jeyaraman, S., Glazier, J. A. & Bacallao, R. L. 2016. Virtual-tissue computer simulations define the roles of cell adhesion and proliferation in the onset of kidney cystic disease. *Mol. Biol. Cell* **27**, 3673–3685 p.mbc.E16-01-0059.
- Bentley, K., Franco, C. A., Philippides, A., Blanco, R., Dierkes, M., Gebala, V., Stanchi, F., Jones, M., Aspalter, I. M., Cagna, G., Weström, S., Claesson-Welsh, L., Vestweber, D. & Gerhardt, H. 2014. The role of differential VE-cadherin dynamics in cell rearrangement during angiogenesis. *Nat. Cell Biol.* **16**, 309–321.
- Boas, S. E. M. & Merks, R. M. H. 2014. Synergy of cell-cell repulsion and vacuolation in a computational model of lumen formation. *J. R. Soc. Interface.* **11**, 20131049.
- Boas, S. E. M. & Merks, R. M. H. 2015. Tip cell overtaking occurs as a side effect of sprouting in computational models of angiogenesis. *BMC Syst. Biol.* **9**, 86.
- Brodland, W. G. 2004. Computational modeling of cell sorting, tissue engulfment, and related phenomena: a review. *Appl. Mech. Rev.* **57**, 47.
- Bryant, D. M. & Mostov, K. E. 2008. From cells to organs: building polarized tissue. *Nat. Rev. Mol. Cell Biol.* **9**, 887–901.
- Carmeliet, P. 2005. Angiogenesis in life, disease and medicine. *Nature* **438**, 932–936.
- Cerruti, B., Puliafito, A., Shewan, A. M., Yu, W., Combes, A. N., Little, M. H., Chianale, F., Primo, L., Serini, G., Mostov, K. E., Celani, A. & Gamba, A. 2013. Polarity, cell division, and out-of-equilibrium dynamics control the growth of epithelial structures. *J. Cell Biol.* **203**, 359–372.
- Chaturvedi, R., Huang, C., Kazmierczak, B., Schneider, T., Izaguirre, J. A., Glimm, T., Hentschel, H. G. E., Glazier, J. A., Newman, S. A. & Alber, M. S. 2005. On multiscale approaches to three-dimensional modelling of morphogenesis. *J. R. Soc. Interface.* **2**, 237–253.
- Chen, B.-C., Legant, W. R., Wang, K., Shao, L., Milkie, D. E., Davidson, M. W., Janetopoulos, C., Wu, X. S., Hammer, J. A., Liu, Z., English, B. P., Mimori-Kiyosue, Y., Romero, D. P., Ritter, A. T., Lippincott-Schwartz, J., Fritz-Laylin, L., Mullins, R. D., Mitchell, D. M., Bembenek, J. N., Reymann, A.-C., Bohme, R., Grill, S. W., Wang, J. T., Seydoux, G., Tulu, U., Serdar, K., Daniel, P. & Betzig, E. 2014. Lattice light-sheet microscopy: imaging molecules to embryos at high spatiotemporal resolution. *Science* **346**, 1257998.
- Cickovski, T. M., Huang, C., Chaturvedi, R., Glimm, T., Hentschel, H., George, E., Alber, M. S., Glazier, J. A., Newman, S. A. & Izaguirre, J. A. 2005. A framework for three-dimensional simulation of morphogenesis. *IEEE/ACM Trans. Comput. Biol. Bioinf.* **2**, 273–287.
- Costantini, F. & Kopan, R. 2010. Patterning a complex organ: branching morphogenesis and nephron segmentation in kidney development. *Dev. Cell* **18**, 698–712.
- Costantini, F. & Shakya, R. 2006. GDNF/Ret signaling and the development of the kidney. *BioEssays* **28**, 117–127.
- Daub, J. T. & Merks, R. M. H. 2013. A cell-based model of extracellular-matrix-guided endothelial cell migration during angiogenesis. *Bull. Math. Biol.* **75**, 1377–1399.
- Daub, J.T. & Merks, R.M.H. 2014. Cell-based computational modeling of vascular morphogenesis using tissue simulation toolkit. *Vasc. Morphog.: Methods Protoc.* **1214**, 67–127.
- Dejana, E. 2004. Endothelial cell-cell junctions: happy together. *Nat. Rev. Mol. Cell Biol.* **5**, 261–270.
- Dias, A. S., de Almeida, I., Belmonte, J. M., Glazier, J. A. & Stern, C. D. 2014. Somites without a clock. *Science* **343**, 791–795.
- Eichmann, A., Yuan, L., Moyon, D., Lenoble, F., Pardanaud, L. & Breant, C. 2005. Vascular development: from precursor cells to branched arterial and venous networks. *Int. J. Dev. Biol.* **49**, 259–267.
- Foty, R. A. & Steinberg, M. S. 2005. The differential adhesion hypothesis: a direct evaluation. *Dev. Biol.* **278**, 255–263.
- Gamba, A., Ambrosi, D., Coniglio, A., de Candia, A., Di Talia, S., Giraudo, E., Serini, G., Preziosi, L. & Bussolino, F. 2003. Percolation, morphogenesis, and burgers dynamics in blood vessels formation. *Phys. Rev. Lett.* **90**, 118101.
- Glazier, J. A. & Graner, F. 1993. Simulation of the differential adhesion driven rearrangement of biological cells. *Phys. Rev. E* **47**, 2128–2154.

- Glazier, J. A., Balter, A. & Poptawski, N. J. 2007. Magnetization to Morphogenesis: A Brief History of the Glazier-Graner-Hogeweg Model. *Single-Cell-Based Models in Biology and Medicine*, 79–106.
- Graner, F. & Glazier, J. A. 1992. Simulation of biological cell sorting using two-dimensional extended Potts model. *Phys. Rev. Lett.* **69**, 2013–2016.
- Grashoff, C., Hoffman, B. D., Brenner, M. D., Zhou, R., Parsons, M., Yang, M. T., McLean, M. A., Sligar, S. G., Chen, C. S., Ha, T. & Schwartz, M. A. 2010. Measuring mechanical tension across vinculin reveals regulation of focal adhesion dynamics. *Nature* **466**, 263–266.
- Harrison, N. C., del Corral, D. R. & Vasiev, B. 2011. Coordination of cell differentiation and migration in mathematical models of caudal embryonic axis extension. *PLoS One* **6**.
- Heisenberg, C.-P. & Bellaïche, Y. 2013. Forces in tissue morphogenesis and patterning. *Cell* **153**, 948–962.
- Hirashima, T., Iwasa, Y. & Morishita, Y. 2009. Dynamic modeling of branching morphogenesis of ureteric bud in early kidney development. *J. Theor. Biol.* **259**, 58–66.
- Hirashima, T., Hosokawa, Y., Iino, T. & Nagayama, M. 2013. On fundamental cellular processes for emergence of collective epithelial movement. *Biol. Open* **2**, 660–666.
- Hogeweg, P. 2000. Evolving mechanisms of morphogenesis: on the interplay between differential adhesion and cell differentiation. *J. Theor. Biol.* **203**, 317–333.
- Jakobsson, L., Franco, C. A., Bentley, K., Collins, R. T., Ponsioen, B., Aspalter, I. M., Rosewell, I., Busse, M., Thurston, G., Medvinsky, A., Schulte-Merker, S. & Gerhardt, H. 2010. Endothelial cells dynamically compete for the tip cell position during angiogenic sprouting. *Nat. Cell Biol.* **12**, 943–953.
- Käfer, J., Hayashi, T., Marée, A. F. M., Carthew, R. W. & Graner, F. 2007. Cell adhesion and cortex contractility determine cell patterning in the *Drosophila* retina. *Proc. Natl Acad. Sci. USA* **104**, 18549–18554.
- Keller, P. J. 2013. Imaging morphogenesis: technological advances and biological insights. *Science (New York, N.Y.)* **340**, 1234168.
- Keller, E. F. & Segel, L. A. 1970. Initiation of slime mold aggregation viewed as an instability. *J. Theor. Biol.* **26**, 399–415.
- Kitano, H. 2002. Systems biology: a brief overview. *Science* **295**, 1662–1664.
- Köhn-Luque, A., de Back, W., Staruß, J., Mattiotti, A., Deutsch, A., Pérez-Pomares, J. M. & Herrero, M. A. 2011. Early embryonic vascular patterning by matrix-mediated paracrine signalling: a mathematical model study. *PLoS One* **6**, e24175.
- Krens, S. F. G. & Heisenberg, C. P. 2011. Cell sorting in development. *Curr. Top. Dev. Biol.* 189–213.
- Krieg, M., Arboleda-Estudillo, Y., Puech, P.-H., Käfer, J., Graner, F., Müller, D. J. & Heisenberg, C.-P. 2008. Tensile forces govern germ-layer organization in zebrafish. *Nat. Cell Biol.* **10**, 429–436.
- Lecuit, T. & Lenne, P.-F. 2007. Cell surface mechanics and the control of cell shape, tissue patterns and morphogenesis. *Nat. Rev. Mol. Cell Biol.* **8**, 633–644.
- Magno, R., Grieneisen, V. A. & Marée, A. F. 2015. The biophysical nature of cells: potential cell behaviours revealed by analytical and computational studies of cell surface mechanics. *BMC Biophys.* **8**, 8.
- Majumdar, A., Vainio, S., Kispert, A., McMahon, J. & McMahon, A. P. 2003. Wnt11 and Ret/Gdnf pathways cooperate in regulating ureteric branching during metanephric kidney development. *Development* **130**, 3175–3185.
- Marée, A. F. M. & Hogeweg, P. 2001. How amoeboids self-organize into a fruiting body: multicellular coordination in *Dicystostelium discoideum*. *Proc. Natl Acad. Sci. USA* **98**, 3879–3883.
- Marée, A.F.M., Grieneisen, V. A & Hogeweg, P. 2007. The Cellular Potts Model and Biophysical Properties of Cells, Tissues and Morphogenesis. *Single-Cell-Based Models in Biology and Medicine*, **2**, 30.
- Martin-Belmonte, F. & Mostov, K. 2008. Regulation of cell polarity during epithelial morphogenesis. *Curr. Opin. Cell Biol.* **20**, 227–234.
- Merks, R. M. H. & Glazier, J. A. 2005. A cell-centered approach to developmental biology. *Phys. A* **352**, 113–130.
- Merks, R. M. H., Brodsky, S. V., Goligorsky, M. S., Newman, S. A. & Glazier, J. A. 2006. Cell elongation is key to in silico replication of in vitro vasculogenesis and subsequent remodeling. *Dev. Biol.* **289**, 44–54.
- Merks, R. M. H., Peryn, E. D., Shirinifard, A. & Glazier, J. A. 2008. Contact-inhibited chemotaxis in de novo and sprouting blood-vessel growth. *PLoS Comput. Biol.* **4**, e1000163.
- Michos, O. 2009. Kidney development: from ureteric bud formation to branching morphogenesis. *Curr. Opin. Genet. Dev.* **19**, 484–490.
- Miyawaki, A. & Niino, Y. 2015. Molecular spies for bioimaging-fluorescent protein-based probes. *Mol. Cell* **58**, 632–643.
- Nakajima, A. & Ishihara, S. 2011. Kinetics of the cellular Potts model revisited. *New J. Phys.* **13**, 33035.
- Newman, M.E.J. & Barkema, G.T. 1999. Monte Carlo Methods in Statistical Physics.
- Noppe, A., Roberts, A. P., Yap, A., Gomez, G. A. & Neufeld, Z. 2015. Modelling wound closure in an epithelial cell sheet using the Cellular Potts Model. *Integr. Biol.* **7**, 1253–1264.
- Oates, A. C., Gorfinkiel, N., Gonzalez-Gaitan, M. & Heisenberg, C. P. 2009. Quantitative approaches in developmental biology. *Nat. Rev. Genet.* **10**, 517–530.
- van Oers, R. F. M., Rens, E. G., LaValley, D. J., Reinhart-King, C. A & Merks, R. M. H. 2014. Mechanical cell-matrix feedback explains pairwise and collective endothelial cell behavior in vitro. *PLoS Comput. Biol.* **10**, e1003774.
- Ouchi, N. B., Glazier, J. A., Rieu, J.-P., Upadhyaya, A. & Sawada, Y. 2003. Improving the realism of the cellular Potts model in simulations of biological cells. *Phys. A* **329**, 451–458.
- Palm, M. M. & Merks, R. M. H. 2013. Vascular networks due to dynamically arrested crystalline ordering of elongated cells. *Phys. Rev. E Stat. Nonlin Soft. Matter Phys.* **87**.
- Pepicelli, C. V., Kispert, A., Rowitch, D. H. & McMahon, A. P. 1997. GDNF induces branching and increased cell proliferation in the ureter of the mouse. *Dev. Biol.* **192**, 193–198.
- Polacheck, W. J. & Chen, C. S. 2016. Measuring cell-generated forces: a guide to the available tools. *Nat. Methods* **13**, 415–423.
- Poptawski, N. J., Swat, M., Scott Gens, J. & Glazier, J. A. 2007. Adhesion between cells, diffusion of growth factors, and elasticity of the AER produce the paddle shape of the chick limb. *Phys. A* **373**, 521–532.
- Prokopiou, S. A., Owen, M. R., Byrne, H. M., Ziyad, S., Domigan, C., Iruela-Arispe, M. L. & Jiang, Y. 2016. Integrative modeling of sprout formation in angiogenesis: coupling the VEGFA-Notch signaling in a dynamic stalk-tip cell selection. arXiv:1606.02167v1.
- Rens, E. G. & Merks, R. M. H. 2017. Cell contractility facilitates alignment of cells and tissues to static uniaxial stretch. *Bioophys. J.* **112**, 755–766.

- Sariola, H. & Sainio, K. 1997. The tip-top branching ureter. *Curr. Opin. Cell Biol.* **9**, 877–884.
- Sasai, Y. 2013. Cytosystems dynamics in self-organization of tissue architecture. *Nature* **493**, 318–326.
- Savill, N. J. & Hogeweg, P. 1997. Modelling morphogenesis: from single cells to crawling slugs. *J. Theor. Biol.* **184**, 229–235.
- Savill, N.J. & Merks, R.M.H., 2007. The Cellular Potts Model in Biomedicine. In *Single-Cell-Based Models in Biology and Medicine*. 14.
- Scianna, M. & Preziosi, L. 2012. Multiscale developments of the cellular Potts model. *Multiscale Model. Simul.* **10**, 342–382.
- Scianna, M., Bassino, E. & Munaron, L. 2015. A cellular Potts model analyzing differentiated cell behavior during in vivo vascularization of a hypoxic tissue. *Comput. Biol. Med.* **63**, 143–156.
- Serwane, F., Mongera, A., Rowghanian, P., Kealhofer, D. A., Lucio, A. A., Hockenbery, Z. M. & Campàs, O. 2016. In vivo quantification of spatially varying mechanical properties in developing tissues. *Nat. Methods* **14**, 181–186.
- Starruß, J., Bley, T., Søgaard-Andersen, L. & Deutsch, A. 2007. A new mechanism for collective migration in *Myxococcus xanthus*. *J. Stat. Phys.* **128**, 269–286.
- Starruß, J., De Back, W., Brusch, L. & Deutsch, A. 2014. Morphus: a user-friendly modeling environment for multiscale and multicellular systems biology. *Bioinformatics* **30**, 1331–1332.
- Steinberg, M. S. 1963. Reconstruction of tissues by dissociated cells. *Science* **141**, 401–408.
- Steinberg, M. S. 2007. Differential adhesion in morphogenesis: a modern view. *Curr. Opin. Genet. Dev.* **17**, 281–286.
- Steinberg, M. S. & Takeichi, M. 1994. Experimental specification of cell sorting, tissue spreading, and specific spatial patterning by quantitative differences in cadherin expression. *Proc. Natl Acad. Sci. USA* **91**, 206–209.
- Sugihara, K., Nishiyama, K., Fukuhara, S., Uemura, A., Arima, S., Kobayashi, R., Köhn-Luque, A., Mochizuki, N., Suda, T., Ogawa, H. & Kurihara, H. 2015. Autonomy and Non-autonomy of angiogenic cell movements revealed by experiment-driven mathematical modeling. *Cell Rep.* **13**, 1814–1827.
- Swat, M. H., Thomas, G. L., Belmonte, J. M., Shirinifard, A., Hmeljak, D. & Glazier, J. A. 2012. Multi-scale modeling of tissues using compucell 3D. *Methods Cell Biol.* **110**, 325–366.
- Szabó, A. & Merks, R. M. H. 2013. Cellular Potts modeling of tumor growth, tumor invasion, and tumor evolution. *Front. Oncol.* **3**, 87.
- Szabo, A., Perryn, E. D. & Czirok, A. 2007. Network formation of tissue cells via preferential attraction to elongated structures. *Phys. Rev. Lett.* **98**, 038102.
- Szabó, A., Varga, K., Garay, T., Hegedűs, B. & Czirok, A. 2012. Invasion from a cell aggregate—the roles of active cell motion and mechanical equilibrium. *Phys. Biol.* **9**, 16010.
- Tang, M. J., Worley, D., Sanicola, M. & Dressler, G. R. 1998. The RET-glia cell-derived neurotrophic factor (GDNF) pathway stimulates migration and chemoattraction of epithelial cells. *J. Cell Biol.* **142**, 1337–1345.
- Townes, P. L. & Holtfreter, J. 1955. Directed movements and selective adhesion of embryonic amphibian cells. *J. Exp. Zool.* **128**, 53–120.
- Zajac, M., Jones, G. L. & Glazier, J. A. 2000. Model of convergent extension in animal morphogenesis. *Phys. Rev. Lett.* **85**, 2022–2025.
- Zajac, M., Jones, G. L. & Glazier, J. A. 2003. Simulating convergent extension by way of anisotropic differential adhesion. *J. Theor. Biol.* **222**, 247–259.